

Activation of CH₄ and H₂ by zirconium(IV) and titanium(IV) cationic complexes. Theoretical DFT study

Yu. A. Ustynyuk *, L. Yu. Ustynyuk, D.N. Laikov, V.V. Lunin

M.V. Lomonosov Moscow State University, Chemistry Department, 119899 Moscow, Vorobyovy gory, Russia

Received 24 July 1999; received in revised form 29 October 1999

Dedicated to Professor Stanislaw Pasynekiewicz on his 70th birthday

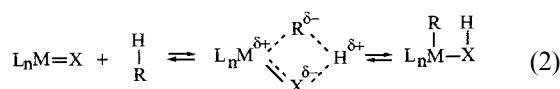
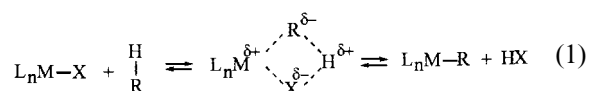
Abstract

The reactions of methane and dihydrogen molecules with the cations $[(\eta^5\text{-C}_5\text{H}_5)_2\text{MCH}_3]^+$ (**1**) and $[(\eta^5\text{-C}_5\text{H}_5)_2\text{MH}]^+$ (**3**) (M = Zr, Ti) have been investigated by gradient-corrected density functional calculations. In the case of CH₄, the active cationic center of **1** or **3** attracts the substrate molecule first to form an agostic complex in which its C–H bond is already somewhat weakened. The σ -bonded ligand exchange reaction in the system **1** + CH₄ proceeds through a symmetric transition state with an activation barrier of 15.0 kcal mol⁻¹ (11.6 kcal mol⁻¹) for the Zr (Ti) complex. Hydrogen reacts with **1** exothermally, $\Delta H_0 = -7.1$ kcal mol⁻¹ (-8.6 kcal mol⁻¹) for Zr (Ti), yielding **3** and CH₄ without an activation barrier. These theoretical results give insight into the mechanism of H/D exchange in methane in the presence of Ziegler–Natta-type catalysts observed experimentally by Grigoryan et al. It is shown that organometallic cationic complexes of Zr(IV) and Ti(IV) may prove to be promising systems for C–H and H–H bond activation under mild conditions. © 2000 Elsevier Science S.A. All rights reserved.

Keywords: Methane C–H bond activation; bis-Cyclopentadienyl zirconium and titanium complexes; H–H bond activation; Density functional calculations

1. Introduction

Selective catalytic activation and functionalization of methane in particular, and alkanes in general, to form useful organic compounds, constitutes an important and complicated problem [1,2]. Homogeneous catalytic systems for the functionalization of alkanes can be classified into three pathways: radical, oxidative addition and electrophilic. Shilov was the first to demonstrate the C–H bond activation by the electrophilic pathway using the Pt(II) ion as the activating species [3]. Four-center activation by transition, lanthanide and actinide metals has been also reported (Eq. (1) [4,5] and Eq. (2) [6]):



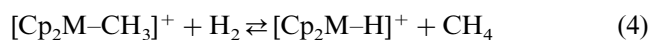
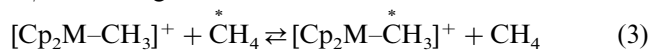
The active catalytic species in the Ziegler–Natta-type olefin polymerization systems are the 16-electron cationic complexes $[\text{L}_n\text{MR}]^+$ (M = Ti, Zr), which can be viewed as coordinatively unsaturated strong Lewis acids. It was shown by Grigoryan [7] that methane-*d*₄ undergoes H/D exchange in the presence of TiCl₄ + Et₂AlCl, (C₅H₅)₂TiCl₂ + Et₂AlCl and (acac)₂TiCl₂ + Et₂AlCl. This is an interesting experimental finding, which awaits proper theoretical explanation. One may suggest that the olefin polymerization and the methane H/D exchange probably proceed through analogous steps and involve similar active species. This hypothesis is supported by the results of detailed theoretical density functional theory (DFT) studies of alkene polymerization by the cationic complexes $[(\eta^5\text{-C}_5\text{H}_5)_2\text{ZrR}]^+$ (R = CH₃, C₂H₅) performed by Ziegler and co-workers [8–11], which have clearly demonstrated the impor-

* Corresponding author. Fax: +7-095-939-2677.

E-mail address: yust@nmr.chem.msu.ru (Y.A. Ustynyuk)

tance of agostic interactions of σ -C–H bonds in alkyl group R with an electron-deficient metal center. Such interactions are well documented and play an important role in many stoichiometric and catalytic reactions [12] of 14 e^- and 16 e^- transition-metal complexes. The ability of alkanes to form σ adducts with metal atoms, ions and complexes is proved in matrix-isolated, solution and gas phases by FTIR, NMR, ICR-MS and other techniques [13–16]. The first complex of a free alkane with an iron(II) porphyrin has recently been characterized by direct X-ray structural investigation [17].

In this paper, we report the results of our DFT study of the gas-phase reactions (3) and (4), which are chosen here as the simplest models of the processes, possibly taking place in the experimentally observable H/D exchange reactions:



M = Zr, Ti

Inspired by the work of Ziegler, we hope that the similar computational method we used would yield results accurate enough to draw certain mechanistic conclusions transferable to reactions in non-polar media as well.

2. Computational details

In the present work, the non-empirical generalized gradient approximation (GGA) for the exchange-correlation functional of Perdew et al. [18] was employed. Its well-documented performance [19], together with its sound physical basis, makes it competitive with, if not superior to, other popular approximations of this type in use. The calculations were performed using the program developed by one of us, which implements an economical computational procedure [20]. Large or-

bital basis sets of contracted Gaussian-type functions of the size (5s1p)/[3s1p] for H, (11s6p2d)/[6s3p2d] for C, (18s13p8d)/[12s9p4d] for Ti and (21s16p12d)/[15s12p7d] for Zr were used in conjunction with the density-fitting basis sets of uncontracted Gaussian-type functions of the size (5s1p) for H, (10s3p3d1f) for C, (18s6p6d5f5g) for Ti and (21s9p9d8f8g) for Zr. The overall accuracy of these basis-set approximations is estimated to be sufficient for the chemical purposes of this work. Full geometry optimization was performed for a number of stable and transition-state structures followed by vibrational frequency calculation using analytical first and second derivatives. Each structure has been characterized by the vibrational analysis and the ΔH_0 values below include the zero-point vibrational correction. The present theoretical method has been used and has given very useful results in the study of some interesting rearrangements in the organometallic chemistry of Cr [21]. To illustrate the performance of this method for the heavier Zr, the calculated geometric parameters of $[\text{Cp}_2\text{Zr}(\text{CH}_3)_2]$ and $[\text{Cp}_2\text{ZrCH}_3]^+$ are listed in Table 1 in comparison with available experimental and theoretical data. One can see that the geometry of both complexes is reproduced rather well.

3. Results and discussion

3.1. The structures of complexes $[\text{Cp}_2\text{MCH}_3]^+$ and $[\text{Cp}_2\text{MH}]^+$

Stationary points have been located on the potential-energy surface (PES) of $[\text{Cp}_2\text{ZrCH}_3]^+$ corresponding to the two stable conformations of the cations **1a** and **2a** (Fig. 1). Both structures possess a symmetry plane crossing the molecule through the zirconium atom, a methyl carbon and one of the three methyl hydrogens. They differ in the orientation of the methyl group relative to this plane. The more stable isomer **1a**

Table 1
Comparison of the calculated geometry parameters for $[\text{Cp}_2\text{Zr}(\text{CH}_3)_2]$ and $[\text{Cp}_2\text{ZrCH}_3]^+$ with experimental data

Parameter (Å, °)	$[\text{Cp}_2\text{Zr}(\text{CH}_3)_2]$		$[\text{Cp}_2\text{ZrCH}_3]^+$		
	Experimental ^a	Calculated	Experimental ^b	Calculated ^c	Calculated
Zr–C _{Me}	2.27	2.30	2.22–2.25	2.18	2.25
Zr–C _{Cp} (avg.)	2.52	2.56	2.52	2.50	2.51
Zr–Cp (centr.)	2.23	2.25	2.21	2.19	2.20
\angle C _{Me} –Zr–C _{Me}	132.6	134.3	–	–	–
\angle Cp–Zr–Cp	95.6	101.1	132.5	138.6	135.4

^a X-ray data [22,23].

^b X-ray data [11,24].

^c Calculations of Woo et al. [11].

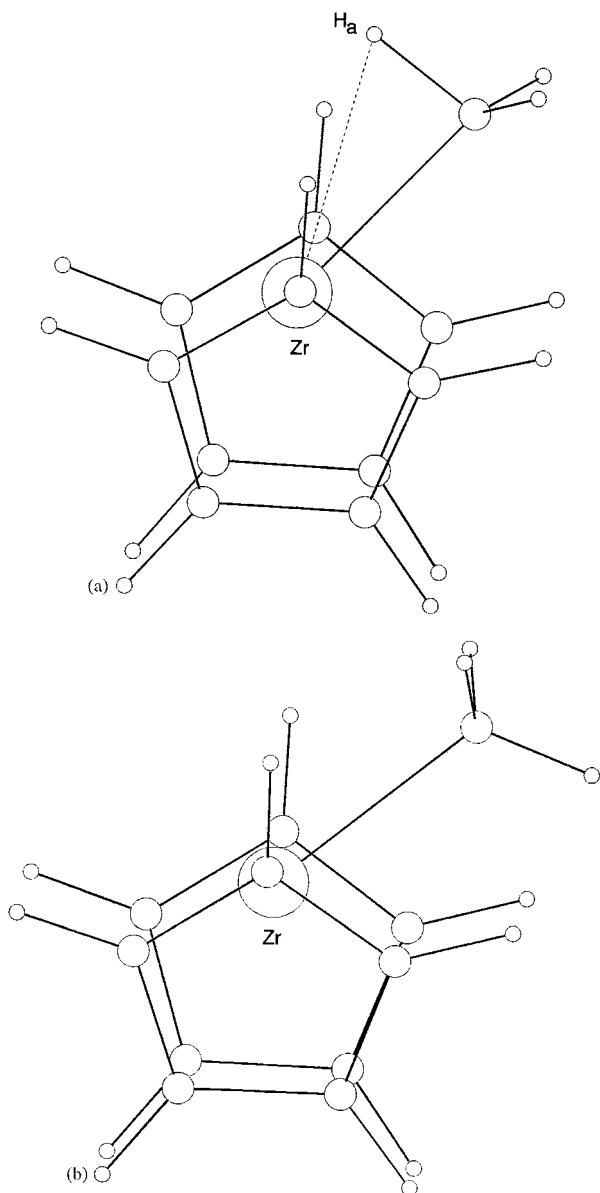


Fig. 1. Optimized structures of $[\text{Cp}_2\text{ZrCH}_3]^+$ isomers **1a** (a) and **2a** (b).

contains an agostic Zr-H_a bond which is shorter (2.39 Å) than the sum of the Zr and H van der Waal's radii (2.5 Å). Accordingly, the Zr-C-H_a bond angle (84°) is more acute and the C-H_a bond distance (1.13 Å) is slightly longer than in ordinary $\text{CH}_3\text{-X}$ fragments. There is no agostic interaction in **2a**. All the Zr-H distances are in the range 2.78–2.96 Å, the bond angles are within $107\text{--}120^\circ$ and all the C-H bonds are about 1.10 Å. But the small energy difference between the two isomers ($\Delta E = 0.44 \text{ kcal mol}^{-1}$), as well as the transition state lying only $0.10 \text{ kcal mol}^{-1}$ higher than **2a**, gives clear evidence that the $[\text{Cp}_2\text{ZrCH}_3]^+$ cation has to be considered as a structure with free rotation of the methyl group around the Zr-CH_3 bond.

Only one stationary point corresponding to the stable **1b** structure with an agostic bond was located on the PES for $[\text{Cp}_2\text{TiCH}_3]^+$, which is very similar to **1a**. The agostic Ti-H_a bond distance is 2.21 Å, the Ti-C-H_a bond angle is 80° and the C-H_a bond distance is 1.13 Å.

The structure of the hydridocation $[\text{Cp}_2\text{MH}]^+$ (**3a**) ($\text{M} = \text{Zr}$) is presented in Fig. 2. The smaller hydrogen ligand leaves much more space in the coordination sphere of the metal in **3** for the coordination of an additional substrate than in **2**. That may be the reason for higher reactivities of hydridocations in comparison with alkyl cationic complexes [25]. Some optimized geometry parameters of complexes **1** and **3** are listed in Tables 2 and 4.

3.2. The mechanism of H/D and $^{12}\text{C}/^{13}\text{C}$ isotope exchanges in the interaction of methane with $[\text{Cp}_2\text{MCH}_3]^+$ cations

The PESs for the model reactions $[\text{Cp}_2\text{MCH}_3]^+ + \text{CH}_4$ ($\text{M} = \text{Zr}, \text{Ti}$) have been studied in some detail. The first step of the interaction is the formation of the intermediate σ complexes **4a** and **4b** (Fig. 3). Their geometry parameters and energies are listed in Tables 2 and 3. Two C-H bonds are involved in the methane binding in the metal's coordination sphere. The complexation energy is higher for the Zr cation ($\Delta H_0 = -7.9 \text{ kcal mol}^{-1}$) than for the Ti one ($\Delta H_0 = -2.0 \text{ kcal mol}^{-1}$). Nevertheless, it has to be emphasized that the free energies of complexation at room temperature, ΔG_{298} , are positive with respect to the separated reagents due to the entropy contributions, and are equal to $1.5 \text{ kcal mol}^{-1}$ for **4a** and to $8.3 \text{ kcal mol}^{-1}$ for **4b** (see Table 3).

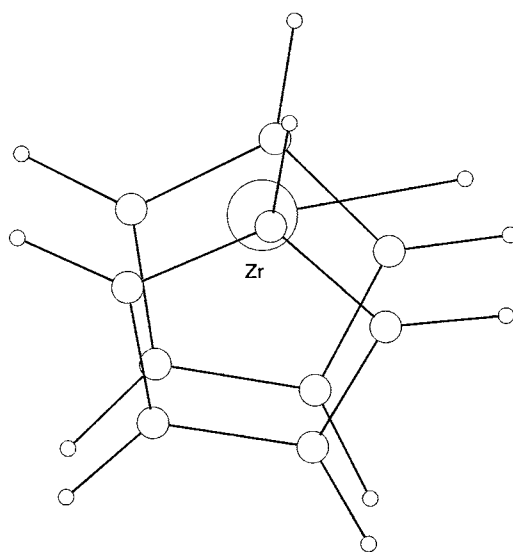


Fig. 2. Optimized structure of $[\text{Cp}_2\text{ZrH}]^+$ (**3a**).

Table 2

Selected geometry parameters of the calculated structures in the reaction $[\text{Cp}_2\text{MC}^*\text{H}_3]^+ + \text{CH}_4 \rightleftharpoons [\text{Cp}_2\text{MCH}_3]^+ + \text{C}^*\text{H}_4$ (M = Zr, Ti)^a

Parameter (Å, °)	1a + CH ₄	4a	5a	1b + CH ₄	4b	5b
M–H ₍₁₎	–	2.40	1.95	–	2.23	1.81
M–C ₍₂₎	–	2.77	2.40	–	2.66	2.31
M–C ₍₃₎	2.23	2.27	2.40	2.10	2.18	2.31
M–H ₍₄₎	2.39	2.92	2.52	2.21	2.77	2.46
M–H ₍₅₎	–	2.37	2.52	–	2.31	2.46
H ₍₁₎ –C ₍₂₎	1.10	1.11	1.45	1.10	1.11	1.43
H ₍₁₎ –C ₍₃₎	–	2.67	1.45	–	2.37	1.43
H ₍₄₎ –C ₍₃₎	1.13	1.10	1.11	1.13	1.10	1.10
C ₍₂₎ –M–C ₍₃₎	–	93	74	–	89	76
C ₍₂₎ –H ₍₁₎ –C ₍₃₎	–	151	177	–	157	178
M–C ₍₂₎ –H ₍₁₎	–	59	54	–	56	51
M–C ₍₃₎ –H ₍₁₎	–	57	54	–	58	51
M–C ₍₂₎ –H ₍₅₎	–	58	83	–	60	85
M–C ₍₃₎ –H ₍₄₎	84	115	83	80	111	85

^a Numbering of atoms from Figs. 3 and 4.

Ligand exchange proceeds as the inner-sphere hydrogen migration from the σ -bonded methane to the methyl ligand. The structure of the transition states **5a** and **5b** is represented in Fig. 4 and some of their optimized geometry parameters are listed in Table 2. The transition state has C_2 symmetry in the case of Zr and C_s symmetry in the case of Ti. The migrating H(1) atom is equidistant from both carbon atoms of the σ -bonded ligands. The interatomic distances H(1)–M are much shorter than those in the intermediate complexes **4** and the sums of van der Waal's radii of metals and hydrogens. These interatomic distances are close to those in hydridocations **3** (see Table 4 for comparison).

The rate constants for the hydrogen migration reactions can be estimated from the data of Table 3 within the Eyring model [26] by the equation:

$$\begin{aligned}
 k &= kT/h \exp(-\Delta G^\ddagger/RT) \\
 &= kT/h \exp(\Delta S^\ddagger/R) \exp(-\Delta H^\ddagger/RT) \\
 &= k_0 \exp(-\Delta H^\ddagger/RT)
 \end{aligned}$$

These values are 20 s^{-1} ($k_0 = 4.4 \times 10^{11} \text{ s}^{-1}$, $\Delta H^\ddagger = 14.2 \text{ kcal mol}^{-1}$) for the Zr complex **4a** and $6 \times 10^3 \text{ s}^{-1}$ ($k_0 = 5.7 \times 10^{11} \text{ s}^{-1}$, $\Delta H^\ddagger = 10.9 \text{ kcal mol}^{-1}$) for the Ti complex **4b**. They should be considered only as rough estimates of possible experimental values for non-polar media, due to some known limitations of the models used.

3.3. Coordination modes and hydrogen exchange in the systems $[\text{Cp}_2\text{MCH}_3]^+ + \text{H}_2$ and $[\text{Cp}_2\text{MH}]^+ + \text{CH}_4$

Two stationary points have been located on the PES of the $[\text{Cp}_2\text{ZrCH}_3]^+ + \text{H}_2$ system, corresponding to the energy minima of stable primary adducts of dihydrogens **6** and **7**. Their structures are presented in Fig. 5. The dihydrogen binding energies in both adducts are much higher than for the methane binding in **4a**. Both complexes **6** and **7** possess the same symmetry plane as the starting $[\text{Cp}_2\text{ZrCH}_3]^+$ does. In the thermodynamically more stable complex **6**, the coordinated dihydrogen molecule is positioned in the symmetry plane. The H–H bond is elongated to 0.82 Å in comparison with 0.75 Å in the intact H_2 molecule. It is noteworthy that a typical agostic bond exists in **6**. According to that, the C–H(4) bond in the methyl ligand is elongated (1.13 Å), the Zr–H(4) bond distance (2.32 Å) is shorter than the van der Waal's radii sum and the Zr–C(3)–H(4) angle is very acute (78°). The geometry of the $\text{Cp}_2\text{Zr}-\text{CH}_3$ core in **6** with respect to the methyl group orientation is quite similar to that in **2a**, in which there is no agostic bond. The energy of a hypothetical structure of $[\text{Cp}_2\text{ZrCH}_3]^+$ derived from **6** by eliminating the coordinated dihydrogen molecule has been calculated to be 2.66 kcal mol⁻¹ higher than that of **2a**. There is no local minimum on the PES of $[\text{Cp}_2\text{ZrCH}_3]^+$ corresponding to this type of structure.

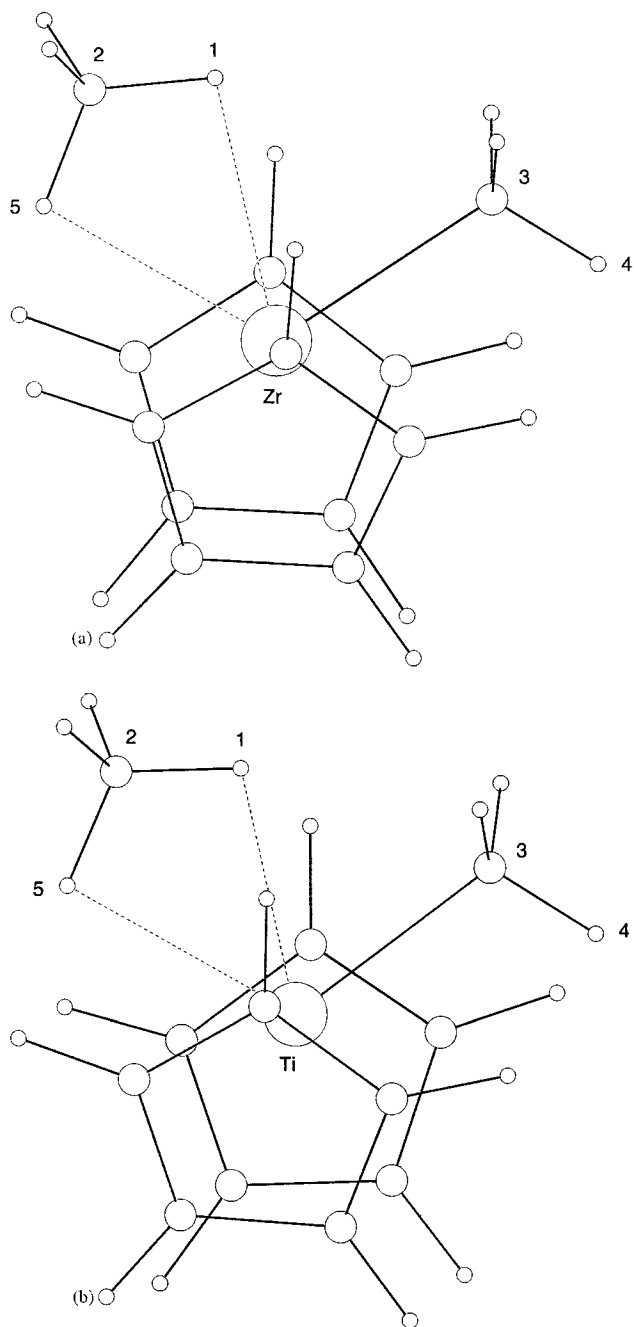


Fig. 3. Optimized structures of the adducts $[\text{Cp}_2\text{M}(\text{CH}_3)\text{CH}_4]^+$ (**4a**) (a) and **4b** (b).

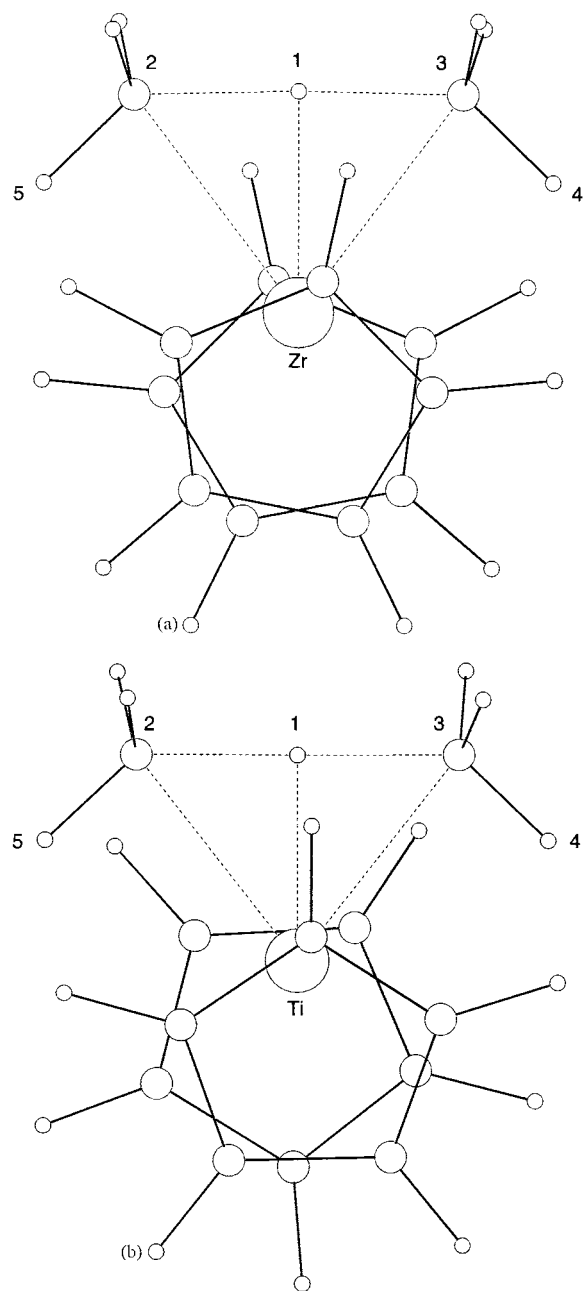


Fig. 4. Optimized structures of the transition states in the reactions $[\text{Cp}_2\text{MCH}_3]^+ + \text{CH}_4$ (**5a**) (a) and **5b** (b).

Table 3

Calculated energetic effects in the reaction $[\text{Cp}_2\text{MC}^*\text{H}_3]^+ + \text{CH}_4 \rightleftharpoons [\text{Cp}_2\text{MCH}_3]^+ + \text{C}^*\text{H}_4$ (M = Zr, Ti)^a

	1a +CH ₄	4a	5a	1b +CH ₄	4b	5b
ΔE (kcal mol ⁻¹)	9.4	0	17.0	4.2	0	13.5
ΔH_0 (kcal mol ⁻¹)	7.9	0	15.0	2.0	0	11.6
ΔH_{298} (kcal mol ⁻¹)	8.0	0	14.2	2.4	0	10.9
ΔS_{298} (cal mol ⁻¹ K ⁻¹)	31.7	0	-5.2	35.9	0	-4.7
ΔG_{298} (kcal mol ⁻¹)	-1.5	0	15.7	-8.3	0	12.3

^a All values are presented with respect to **4a** for M = Zr or to **4b** for M = Ti.

Table 4

Selected geometry parameters of the calculated structures in the reaction $[\text{Cp}_2\text{MCH}_3]^+ + \text{H}_2 \rightleftharpoons [\text{Cp}_2\text{MH}]^+ + \text{CH}_4$ (M = Zr, Ti)^a

Parameter (Å, °)	1a+H ₂	6	8	9a	3a+CH ₄	1b+H ₂	9b	3b+CH ₄
M–H ₍₁₎	–	2.04	1.96	2.27	–	–	2.09	–
M–H ₍₂₎	–	2.08	1.98	1.83	1.82	–	1.69	1.68
M–C ₍₃₎	2.23	2.27	2.33	2.70	–	2.10	2.53	–
M–H ₍₄₎	2.39	2.32	2.36	2.39	–	2.21	2.24	–
H ₍₁₎ –H ₍₂₎	0.75	0.82	0.91	2.11	–	0.75	1.95	–
H ₍₁₎ –C ₍₃₎	–	1.99	1.66	1.12	1.10	–	1.12	1.10
H ₍₄₎ –C ₍₃₎	1.13	1.13	1.13	1.11	1.10	1.13	1.11	1.10
H ₍₂₎ –M–C ₍₃₎	–	78	71	85	–	–	87	–
H ₍₂₎ –H ₍₁₎ –C ₍₃₎	–	150	157	150	–	–	149	–
M–H ₍₂₎ –H ₍₁₎	–	75	75	70	–	–	70	–
M–C ₍₃₎ –H ₍₁₎	–	57	56	56	–	–	55	–
M–C ₍₃₎ –H ₍₄₎	120	78	78	62	–	80	62	–

^a Numbering of atoms from Figs. 5–7.

In the less stable complex **7**, the coordinated H₂ molecule is positioned perpendicular to the symmetry plane, the Zr–H bond distances are slightly longer (2.25 Å) and the H(1)–H(2) bond distance is shorter (0.78 Å) in comparison with **6**. There is no agostic interaction between the Zr atom and the C–H bonds of the methyl ligand. The energy difference between **6** and **7** is 1.4 kcal mol^{−1}.

The transformation of **7** to **6** proceeds by the 90° rotation of the H₂ molecule in the coordination sphere concerted with its displacement towards the methyl ligand. The agostic bond Zr–H(4) is formed in this process simultaneously. The transition state for the transformation of **7** to **6** has been located with an energy only 1.2 kcal mol^{−1} higher than **7** and 2.6 kcal mol^{−1} higher than **6**. Inclusion of the vibrational corrections lowers these values to 1.0 and 0.4 kcal mol^{−1}, respectively. Thus, this H₂ adduct has a really fluxional structure.

Among primary dihydrogen complexes **6** and **7**, only the more stable **6** is lying on the reaction path for inner-sphere hydrogen atom migration. Rather small displacements in the coordinated H₂-molecule and methyl ligand are necessary to reach an ‘early’ transition state **8** (see Fig. 6). The concerted elongation of the H(1)–H(2) bond and the shortening of the H(1)–C(3) distance are most essential. This region of the PES is very flat, and the energy difference separating **6** from the transition state **8** is only 0.5 kcal mol^{−1}, or even 0.03 kcal mol^{−1} with the vibrational correction (see Table 5). It means that the transformation of **6** into the final product $[\text{Cp}_2\text{Zr}(\text{H})\text{CH}_4]^+$ (**9a**) proceeds without an activation barrier, or to put it more clearly, the structure **6** does not exist at all and the interaction of H₂ with the cation **1a** leads directly to **9a**.

The structure of **9a** which corresponds to the global energy minimum on the PES under study is repre-

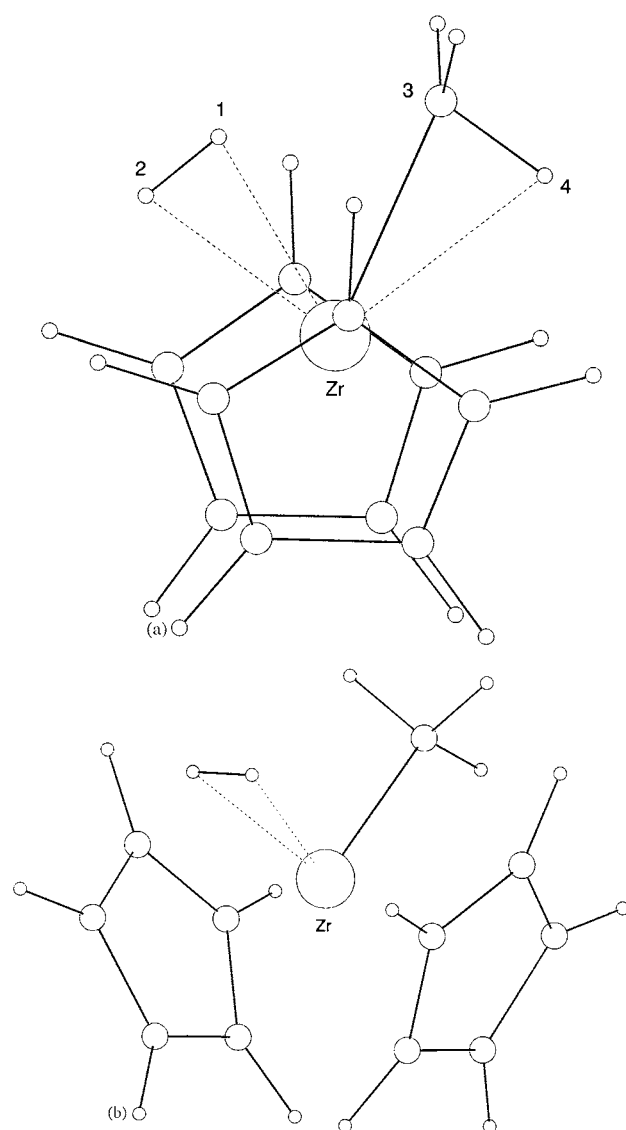
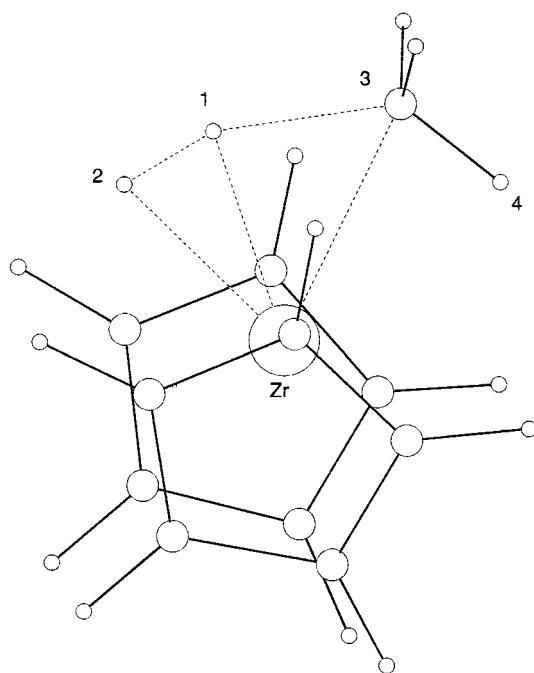
Fig. 5. Optimized structures of the adducts $[\text{Cp}_2\text{Zr}(\text{CH}_3)\text{H}_2]^+$ (**6**) (a) and **7** (b).

Table 5

Calculated energetic effects in the reaction $[\text{Cp}_2\text{MCH}_3]^+ + \text{H}_2 \rightleftharpoons [\text{Cp}_2\text{MH}]^+ + \text{CH}_4$ (M = Zr, Ti)^a

	1a + H ₂	6	8	9a	3a + CH ₄	1b + H ₂	9b	3b + CH ₄
ΔE (kcal mol ⁻¹)	23.2	13.6	14.1	0	12.0	23.3	0	10.8
ΔH_0 (kcal mol ⁻¹)	17.8	12.0	12.0	0	10.7	17.3	0	8.7
ΔH_{298} (kcal mol ⁻¹)	19.2	11.7	11.4	0	10.9	18.8	0	9.3
ΔS_{298} (cal mol ⁻¹ K ⁻¹)	26.1	-3.4	-5.0	0	32.3	30.1	0	36.8
ΔG_{298} (kcal mol ⁻¹)	11.4	12.7	12.9	0	1.3	9.9	0	-1.7

^a All values are given with respect to **9a** for M = Zr and to **9b** for M = Ti.Fig. 6. Optimized structure of the transition state **8** in the reaction $[\text{Cp}_2\text{ZrCH}_3]^+ + \text{H}_2$.

sented in Fig. 7; its geometry parameters and energies are listed in Tables 4 and 5. The methane coordination mode is quite similar to that in **4a**.

For the interaction of $[\text{Cp}_2\text{TiCH}_3]^+$ (**1b**) with dihydrogen, neither intermediate complexes like **6** or **7** nor transition states were located on the PES. The only stationary point detected corresponds to the methane σ complex $[\text{Cp}_2\text{Ti}(\text{H})\text{CH}_4]^+$ (**9b**). It means that the reaction proceeds without an activation barrier. The driving force of the process is its high exothermicity ($\Delta H_0 = -17.3$ kcal mol⁻¹). Endothermic dissociation of **9b** into **3b** and CH₄ is favored by substantial entropy gain. Thus, the comparison of the reactions of $[\text{Cp}_2\text{MCH}_3]^+$ (M = Zr, Ti) cations with dihydrogen shows clearly that **1b** is a bit more reactive towards H₂ than **1a**.

4. Conclusions

The data presented above confirm the high Lewis acidity of the cationic complexes $[\text{Cp}_2\text{MR}]^+$ (M = Zr, Ti, R = H, CH₃) and their ability to coordinate methane and dihydrogen. The binding energy of methane in the $[\text{Cp}_2\text{Zr}(\text{CH}_3)\text{CH}_4]^+$ adduct is 7.9 kcal mol⁻¹. It is comparable to the binding energy of ethylene in $[\text{Cp}_2\text{Zr}(\text{CH}_3)\text{C}_2\text{H}_4]^+$, which is 17.0 kcal mol⁻¹ according to our recent calculation. The fact that H₂ reacts with $[\text{Cp}_2\text{ZrCH}_3]^+$ exothermically and without an activation barrier explains why dihydrogen in small quantities is practically used as an efficient chain terminator [27] for the regulation of polyolefin molecular mass in the Ziegler–Natta type polymerization processes.

In general, our theoretical data are in good agreement with Grigoryan's qualitative experimental facts about the H/D isotope exchange in methane-*d*₄ [7]. His hypothetical mechanism, where the formation of the complex $\text{Cp}_2\text{Zr}=\text{CH}_2$ is the key point, is most probably not in operation, but a more detailed study of this pathway is needed for a final conclusion to be drawn.

The electrophilic activation of methane and probably some other alkanes by $[\text{Cp}_2\text{MR}]^+$ M = Ti, Zr, could be compatible with some further modification with oxidants. Therefore, it should be possible, at least in principle, to design a catalytic oxidation procedure that is based on such an electrophilic C–H cleavage step. The study of the coordination of other donor molecules by the $[\text{Cp}_2\text{MR}]^+$ system is now in progress in our group.

Acknowledgements

This work was supported by the State programs 'Universities of Russia — Basic Research' (grant no. 5223), 'Leading scientific schools of Russia' (grant no. 96-15-97469), Russian Foundation for Basic Research (grant no. 99-03-32792) and by the Special State research program 'Ecology safe processes

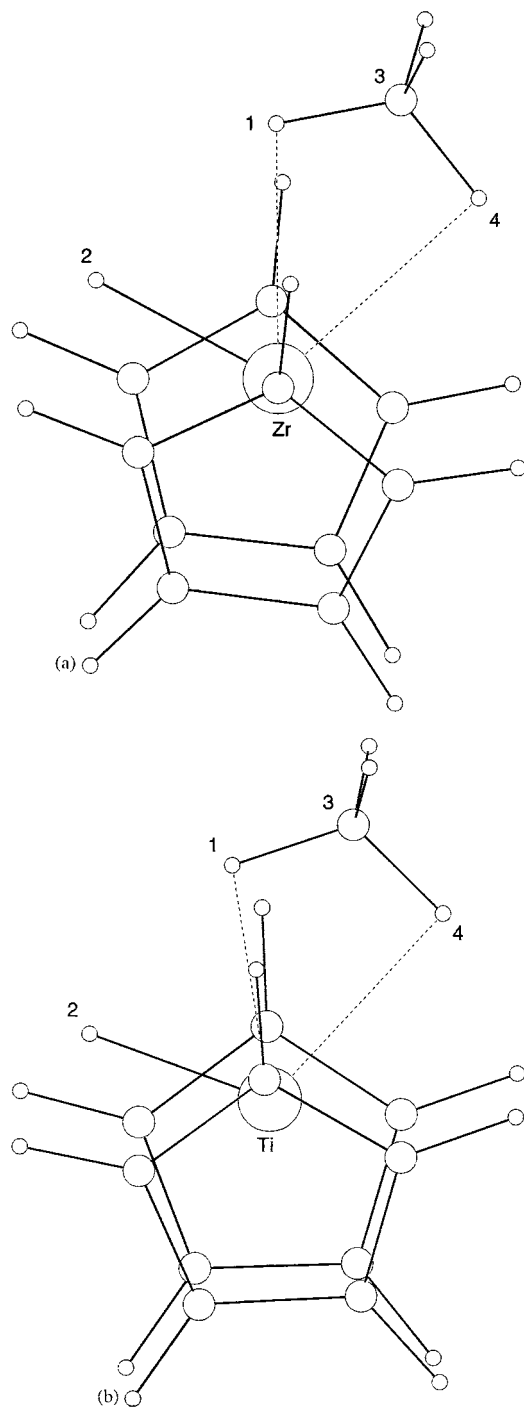


Fig. 7. Optimized structures of the complexes $[\text{Cp}_2\text{M}(\text{H})\text{CH}_4]^+$ (**9a**) (a) and **9b** (b).

in chemistry and chemical technology'. The authors are grateful to Professor B.M. Bulychev, Dr V.I. Pupyshchev, D.A. Tyurin and Dr V.L. Yarnykh for fruitful discussions and assistance in preparing this paper.

References

- [1] R.H. Crabtree, *Chem. Rev.* 95 (1995) 987.
- [2] A.E. Shilov, G.B. Shul'pin, *Chem. Rev.* 97 (1997) 2879.
- [3] A.E. Shilov, *Activation of Saturated Hydrocarbons by Transition Metal Complexes*, Reidel, Dordrecht, 1985.
- [4] M.E. Thompson, S.M. Baxter, A.R. Bulls, B.J. Burger, M.S. Nolan, B.D. Santasiero, W.P. Schaefer, J.E. Bercaw, *J. Am. Chem. Soc.* 109 (1987) 203.
- [5] P.L. Watson, *J. Am. Chem. Soc.* 105 (1983) 6491.
- [6] C.M. Fendrick, T.J. Marks, *J. Am. Chem. Soc.* 108 (1986) 425.
- [7] E.A. Grigoryan, *Uspekhi Khim.* 53 (1984) 347.
- [8] P. Margl, L. Deng, T. Ziegler, *Organometallics* 17 (1998) 933.
- [9] P. Margl, J.C.W. Lohrenz, T. Ziegler, P. Blöchl, *J. Am. Chem. Soc.* 118 (1996) 4434.
- [10] J.C.W. Lohrenz, T.K. Woo, T. Ziegler, *J. Am. Chem. Soc.* 117 (1995) 12793.
- [11] T.K. Woo, L. Fan, T. Ziegler, *Organometallics* 13 (1994) 2252.
- [12] G.L. Soloviechik, *Metallorg. Khim.* 11 (1987) 513.
- [13] C. Hall, R.N. Penetz, *Chem. Rev.* 96 (1996) 3125.
- [14] X.Z. Sun, D.C. Grills, S.M. Nikiforov, M. Poliakoff, M.W. George, *J. Am. Chem. Soc.* 119 (1997) 7521.
- [15] C.L. Gross, G.S. Girolami, *J. Am. Chem. Soc.* 120 (1998) 6605.
- [16] S. Geftakis, G.E. Ball, *J. Am. Chem. Soc.* 120 (1998) 9953.
- [17] D.R. Evans, T. Drovetskaya, R. Bau, C.A. Reed, P.D.W. Boyd, *J. Am. Chem. Soc.* 119 (1997) 3633.
- [18] J.P. Perdew, K. Burke, M. Ernzerhof, *Phys. Rev. Lett.* 77 (1996) 3865.
- [19] M. Ernzerhof, G.E. Scuseria, *J. Chem. Phys.* 110 (1999) 5029.
- [20] D.N. Laikov, *Chem. Phys. Lett.* 281 (1997) 151.
- [21] O.I. Trifonova, E.A. Ochertyanova, N.G. Akhmedov, V.A. Roznyatovsky, D.N. Laikov, N.A. Ustynyuk, Yu.A. Ustynyuk, *Inorg. Chim. Acta* 280 (1998) 328.
- [22] L.E. Schock, C.P. Brock, T.J. Marks, *Organometallics* 6 (1987) 232.
- [23] W.E. Hunter, D.C. Hrncir, R. Vann Bynum, R.A. Penttila, J.L. Atwood, *Organometallics* 2 (1983) 750.
- [24] X. Yang, C.L. Stern, T.J. Marks, *J. Am. Chem. Soc.* 113 (1991) 3623.
- [25] X. Yang, C.L. Stern, T.J. Marks, *J. Am. Chem. Soc.* 116 (1994) 10015.
- [26] S. Glasstone, K.J. Laidler, H. Eyring, *The Theory of Rate Processes*, first ed., New York and London, 1941, p. 24.
- [27] D.E. Richardson, N.G. Alameddini, M.F. Ryan, T. Hayes, J.R. Eyler, A.R. Siedle, *J. Am. Chem. Soc.* 118 (1996) 11244.